Korea-Australia Rheology Journal
Vol. 13, No. 3, September 2001 pp. 141-148

Experimental studies on the axisymmetric sphere-wall interaction in Newtonian and non-Newtonian fluids

Sang Wang Lee, Sun-Mo Sohn, Seung Hee Ryu, Chongyoup Kim*[1] and Ki-Won Song**
Department of Polymer Engineering, Chungnam National University, Taejon, Korea
***School of Chemical Engineering, Pusan National University, Pusan 609-735, Korea*
(Received August 21, 2001; final revision received August 28, 2001)

Abstract

In this research, experimental studies have been performed on the hydrodynamic interaction between a spherical particle and a plane wall by measuring the force between the particle and wall. To approach the system as a resistance problem, a servo-driving system was set-up by assembling a microstepping motor, a ball screw and a linear motion guide for the particle motion. Glycerin and dilute solution of polyacrylamide in glycerin were used as Newtonian and non-Newtonian fluids, respectively. The polymer solution behaves like a Boger fluid when the concentration is 1,000 ppm or less. The experimental results were compared with the asymptotic solution of Stokes equation. The result shows that fluid inertia plays an important role in the particle-wall interaction in Newtonian fluid. This implies that the motion of two particles in suspension is not reversible even in Newtonian fluid. In non-Newtonian fluid, normal stress difference and viscoelasticity play important roles as expected. In the dilute solution weak shear thinning and the migration of polymer molecules in the inhomogeneous flow field also affect the physics of the problem.

Keywords **:** hydrodynamic interaction, shear thinning, first normal stress difference, inertia, migration, wall slip

1. Introduction

The flow of solid suspension and particle motion in the suspension have been of great interest in the materials development and industrial processes such as rocket propellants, high strength ceramics and reinforced polymer composites. There have been growing interests on the microstructure of particles in the suspension since the material properties are largely determined by the microstructure developed through the migration of particles in suspension. Until now, most studies have been focused on suspensions dispersed in Newtonian fluids except a few cases (e.g. Tehrani *et al.*, 1996; Jefri and Zahed, 1990; Huang *et al.*, 1997, Kim *et al.*, 2000; Kim, 2001). However, in many practical cases, viscoelastic liquids are used as the dispersing medium.

The macroscopic migration of particles in suspension is caused by the approach or separation of two particles in suspension. Therefore, to understand the particle migration in suspension, it is necessary to understand the hydrodynamic interaction among particles. The theory of two-particle interaction in Stokes regime of Newtonian fluid has been well documented in Kim and Karrila (1990) and Yang and Park (1998). The problem of three-particle interaction does not have a general solution yet. In this case, one can use the pairwise additivity or numerical solutions if necessary. When the fluid is non-Newtonian, even a single particle problem has some controversial results. For example, in the case of a Boger fluid, both the drag reduction and enhancement have been reported as the Weissenberg number ($We=\lambda\dot{\gamma}$) increases while Reynolds number is kept sufficiently small (Solomon and Muller, 1996 and references therein). But Oldroyd-B model predicts drag reduction that is widely used as the constitutive equation for Boger fluid. Recently Solomon and Muller (1996) reported that the difference was caused by the different extensional characteristics. Studies on the particle-particle interaction in non-Newtonian fluid have been quite rare in spite of its importance in suspension rheology (Brunn, 1977). Especially experimental studies have not been reported yet as far as the authors are aware of. Recently, Patankar and Hu (2001) considered the rheology of suspension of particles theoretically in second order fluid and Oldroyd-B fluid.

*Corresponding author: cykim@grtrkr.korea.ac.kr
[1]Present address: Department of Chemical Engineering and Applied Rheology Center, Korea University

2. Particle-wall interaction in Newtonian fluid

The hydrodynamic interaction between a particle and a solid wall is also an important topic in understanding the flow of suspension macroscopically, especially in relation to wall slip. The hydrodynamic interaction between a particle and a wall is a special case of particle-particle interaction with one particle having an infinitely large diameter. Hence the problem can be considered as a hydrodynamic interaction between two particles with different diameter. The relative motion between a particle and a plane wall can be divided into the following three independent modes:

1) The particle moves parallel to the solid wall
2) The particle approaches to the wall axisymmetrically
3) The particle moves away from the wall axisymmetrically

In the case of Stokes flow, modes 2) and 3) are not independent and are just the reversal of each other. However, in the case of polymer solution, the biaxial flow 2) and the extensional flow 3) are basically different. In this study, we investigated axisymmetric cases of 2) and 3) by measuring the force exerted on the particle.

In concentrated suspension, the average distance between two particles is given as follows (Barnes *et al.*, 1989):

$$\frac{h}{d}=\left(\frac{1}{3\pi\phi}+\frac{5}{6}\right)^{1/2}-1=2\varepsilon \tag{1}$$

where h and $d = 2a$ denote the shortest distance between two particles and the diameter of particle, respectively, and ϕ is the particle loading. When the particle loading is 50%, the average distance between two particles is 0.023 times the diameter. When the particle loading is 30%, this value is 0.090. Therefore in concentrated suspension, the distance between particles is much shorter than the particle diameter. This means that we need to consider the case of small gap problems. Also, the average distance between a particle and a solid wall should have almost the same magnitude.

In the case of a narrow gap problem in Newtonian fluid (See Fig. 1.), the force F between two particles can be determined by applying the lubrication approximation and is given as an asymptotic solution while using ε as the small parameter as follows (Kim and Karrila, 1990):

$$\frac{F}{6\pi\mu aU}=\frac{\beta^2}{(1+\beta)^2}\varepsilon^{-1}-\frac{(1+7\beta+\beta^2)}{5(1+\beta)^3}\ln\frac{1}{\varepsilon}+K(\beta)$$

$$-\frac{(1+18\beta-29\beta^2+18\beta^3+\beta^4)}{21(1+\beta)^4}\varepsilon\ln\frac{1}{\varepsilon}+O(\varepsilon) \tag{2}$$

where β is the ratio of the radii of two particles (b/a = radius of the stationary particle/radius of the test particle), μ is the viscosity of liquid, U is the velocity of the approaching particle. In the above equation, $K(\beta)$ has to be determined by matching with the outer solution. In other words, we need to know the macroscopic motion of the particle. In the following we will use the force determined from Eqn. (2) as the reference value in considering the non-Newtonian case. To calculate the force between a particle and a wall, we can simply set $\beta=\infty$ in Eqn. (2).

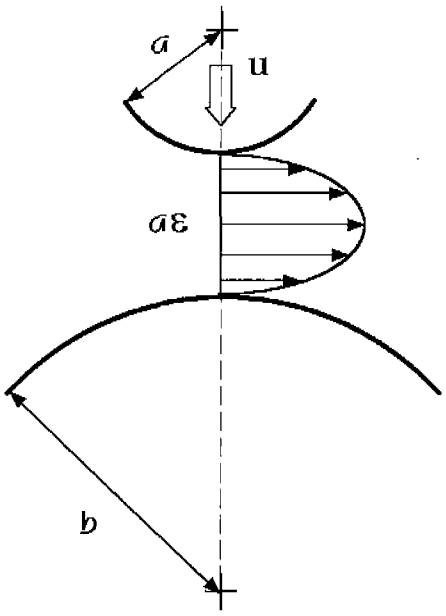

Fig. 1. Hydrodynamic interaction between two spherical particles.

Even though the nature of the particle motion follows that of the mobility problem in suspension, it is hardly possible to simulate such a motion experimentally. Therefore we decided to study the problem by a resistance problem. In this case, we can arbitrarily move particles and measure the force. The experiment is possible by using a computer-controlled servo- or micro-stepping motor together with very accurate linear motion guides. Through the study of this resistance problem, we may gain some insight on the effect of non-Newtonian rheology in suspension.

3. Experimental

As the non-Newtonian fluid, dilute solutions of polyacrylamide in glycerin were used. Polyacrylamide was obtained from Aldrich Chem. Co. (Catalog No.: 18,327; Molecular weight: 5,000,000) and used as received. First a master solution of 1000 ppm was prepared. More dilute solution was prepared by adding more glycerin as desired.

The rheological properties of polymer solution were measured using the Couette or cone-and-plate fixtures of ARES from Rheometrics Inc. In Fig. 2, the viscosity is plotted against shear rate for differing polymer concentrations. The fluid exhibits the typical behavior of Boger fluid: For three decades of shear rate, the viscosity shows almost no shear thinning and the change in viscosity does not exceed more than 36% in the experimental ranges con-

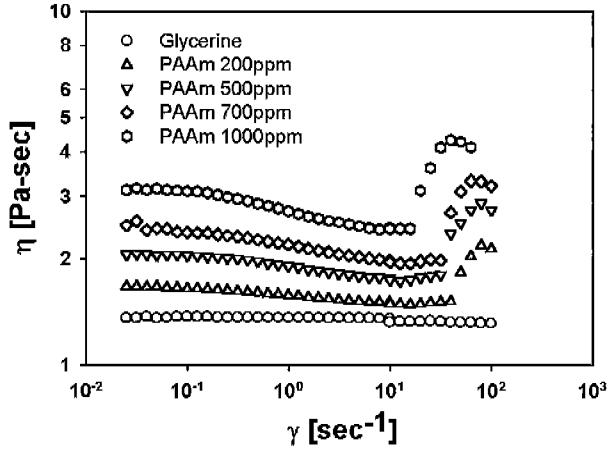

Fig. 2. Viscosity of polyacrylamide solution. The solvent is glycerin. When the concentration of polymer is less than 1000 ppm, the solution behaves as a Boger fluid. The abrupt change in viscosity is caused by the elastic instability in the Couette flow.

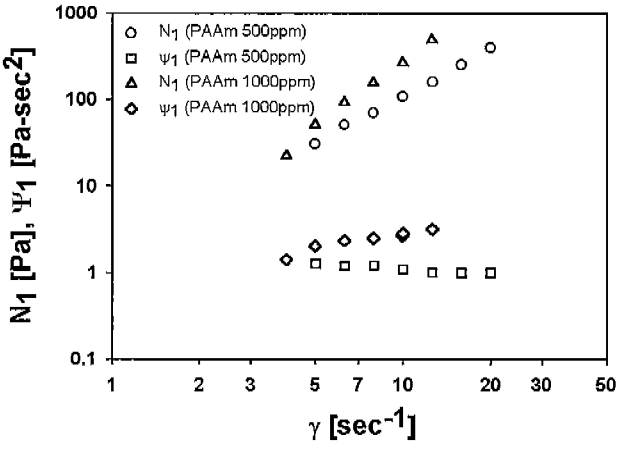

Fig. 3. First normal stress and first normal stress coefficient of polyacrylamide solution. The solvent is glycerin.

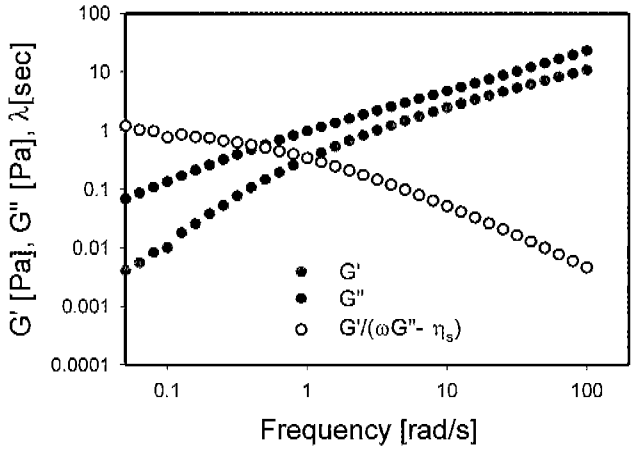

Fig. 4. Storage and loss moduli of 1000ppm solution of polyacrylamide in glycerin. The dynamic behavior is typical of a dilute polymer solution. The time constant of the solution was determined by extrapolating $G'/(\omega G''-\eta_s)$ to zero frequency.

sidered here. The abrupt increases in viscosity when shear rate becomes larger than 10 sec^{-1} appear to be due to elastic instability of Boger fluid (Larson, 1992; Shaqfeh, 1996). The same phenomenon was also reported by Dontula *et al.* (1999) for dilute solutions of polyethylene oxide in polyethylene glycol. In Fig. 3, the first normal stress difference (N_1) and the first normal stress difference coefficient (Ψ_1) are plotted. Due to the instrumental limit, N_1 was measured only in the shear rate ranges shown in Fig. 3. As expected, N_1 is proportional to $\dot{\gamma}^2$ and Ψ_1 is constant for the shear rate range. But we have to be careful whether this constant value is truly zero-shear first normal stress difference coefficient (Ψ_{10}) since Boger fluids could have the 2nd plateau in Ψ_1 (Shaqfeh, 1996). Fig. 4 shows G' and G'' of 1000ppm solution. As $\omega \to 0$, the slopes of G' and G'' tend to 2 and 1, respectively. This is typical behavior of dilute polymer solution. By comparing the time constant from the linear viscoelastic data ($\lambda = \lim_{\omega \to 0} \eta''/\eta_p\omega$) with the value determined from the viscometric data ($\lambda = \lim_{\gamma \to 0} \Psi_1/2\eta_p$), we could confirm that the plateau value was Ψ_{10}. The time constants of 200, 500, 700 and 1000ppm solutions were 1.9, 1.9, 1.95 and 2.5 seconds, respectively. This means that the 1000 ppm solution is slightly over the dilute limit.

Fig. 5 shows the flow system used in this study. The system is composed of a servo-driving linear motion system, a reservoir, a load cell, an argon laser (Lexel Model 25, 0-800 mW) and the sphere. The Ar laser was installed for further studies using flow visualization and particle image velocimetry. The servo-driving linear motion system was set-up by assembling a micro-stepping motor (Parker Compumotor S83_93_Mo), a ball screw and a linear motion guide (Parker 404XR). The resolution of the micro-stepping motor was set at 25,000 steps/revolution for smooth movement. The maximum length of movement was 800 mm. The reservoir was made from glass. It has the dimension of 250 mm× 250 mm× 400 mm. Parallel to the lower plate, a circular plate was attached as the solid wall. The load cell was purchased from CAS Co. Ltd., Korea (MW-120). The maximum load was 120 g. The analog data from the load cell was collected every 0.02 sec by a data acquisition system (HP 34970A). The sphere was machined from Plexiglas. The diameter of the sphere was 50 mm and the variation in diameter was controlled within 100 microns and the surface roughness was controlled within 5 microns. The solid wall (the circular plate) was also made from Plexiglas. Its diameter was 100 mm. The sphere was hanged by a piece of 1mm steel string to the load cell. The sphere was placed axisymmetrically to the circular plate. Since the string has to be immersed in the fluid, it exerts extra force to the load cell due to buoyancy and drag. Also,

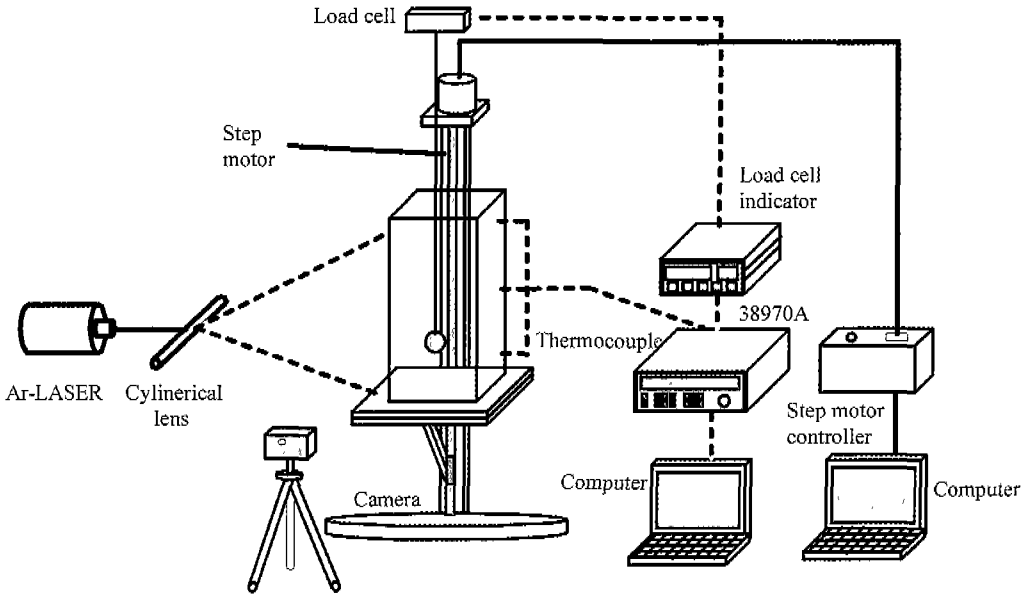

Fig. 5. Schematic diagram of the experimental apparatus.

at the air/liquid interface, a coating flow develops when the reservoir is pulled down and a dipping flow develops when the reservoir is pushed up. Therefore we needed to consider these two problems properly. To determine the net drag force exerted on the sphere, the force was also measured without hanging the sphere and the difference between the forces with and without the sphere was calculated. The zero point of the sphere location was determined while moving the reservoir little by little. It was regarded that the sphere touches the wall when the load cell signal increases abruptly.

The reservoir was set into a sinusoidal oscillation so that the shortest distance d between the particle and the wall (plate) is given as follows:

$$\frac{h}{d} = \varepsilon_0 + p(1+\sin\omega t) \tag{3}$$

In the above equation ω is angular velocity, p is amplitude and ε_0 is the minimum approach.

To validate the equipment and data-processing procedure, we first investigate the translation of a single sphere in a Newtonian fluid. The flow around a sphere is one of the most fundamental problems in fluid mechanics and the solution is well known Stokes solution when the inertia of fluid is negligible. The wall effect is well documented in Happel and Brenner (1983). In the case of a flow around Boger fluid, both increase and decrease in drag from the Newtonian value are reported in the literature depending on the kinds of Boger fluids. This difference is known to arise from the different extensional characteristics of different Boger fluids (Solomon and Muller, 1996).

In Fig. 6, drag coefficient (C_D) is plotted against Reynolds number. In the case of Newtonian fluid, the experimentally determined C_D is fitted to the theoretical value corrected by the wall effect as follows (Happel and Brenner, 1983):

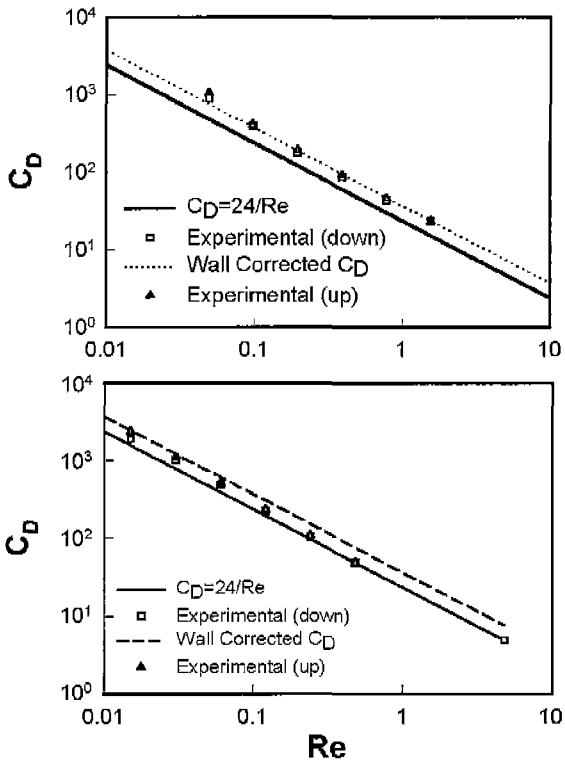

Fig. 6. Drag coefficient of a single sphere in glycerin and 1000 ppm polyacrylamide solution. Upper: glycerin; Lower: polymer solution. The wall corrected value was obtained by assuming that the the container has a circular cross section with the same area.

$$C_{D,\ wall\ corrected} = C_{D,\ Stokes\ Solution} K_1$$

$$K_1 = \frac{1-0.75857(a/R_0)^5}{1-2.1050(a/R_0)+2.0865(a/R_0)^3+0.72603(a/R_0)^6} \quad (4)$$

where a and R_0 are the radii of the particle and the container, respectively. In our experimental system the radius of the container was estimated by assuming that the container has a cylindrical shape with the diameter of the same cross sectional area. From the good fit, we regarded that the experimental method was validated including the methods of the wall correction and the correction for the hanging string.

The experimental conditions have been chosen so that the Reynolds number and Weissenberg number have the same orders of magnitude as the values in a flowing suspension at a typical condition as follows: We consider a shear flow of suspension with shear rate 20 sec^{-1}. The particle loading is 0.5. The average particle diameter is 100 micrometer and the viscosity of the suspending liquid is 1 mPa.s. It is assumed that the particles in a concentrated suspension undergoing a shearing motion move affinely and the number of collisions experienced by a test particle is given by $K\dot{\gamma}\phi$, where the constant K has an order of unity (Phillips et al., 1992). Then the average number of collisions per particle (f) in the above condition is 10 sec^{-1} and the Reynolds number is

$$Re = \frac{D^2 f \rho}{\mu} = 0.1 \quad (5)$$

This value may be thought to be large for suspensions of very small particles under near stagnant conditions. However, it is known that Reynolds number could be even larger than this value in the processing of colloids such as transportation, dispersing of particles in colloid or pearl mills, stirred vessels and so on (Folkersma, *et al.*, 2000). To have approximately the same value of Re in the experiment, we can choose D = 30 mm, μ = 5Pa.s, ω = 0.5 for the sinusoidal motion. Considering the uncertainty in K, we may consider that the experimental condition chosen here is similar to the condition of the particle collision in a suspension under shearing flow.

4. Result and Discussion

In Fig. 7, the force exerted on the stationary particle due to the oscillatory movement of the wall in Newtonian fluid is plotted when the period of oscillation is 10 seconds. In this case the average particle separation is chosen so that it is the same as the distance between two neighboring particles in a dense suspension when the particle loading is 30% and the approach of the particle to the wall is 30% of the average gap size. When the plate begins to move down, fluid rushes into the very narrow gap between the wall and

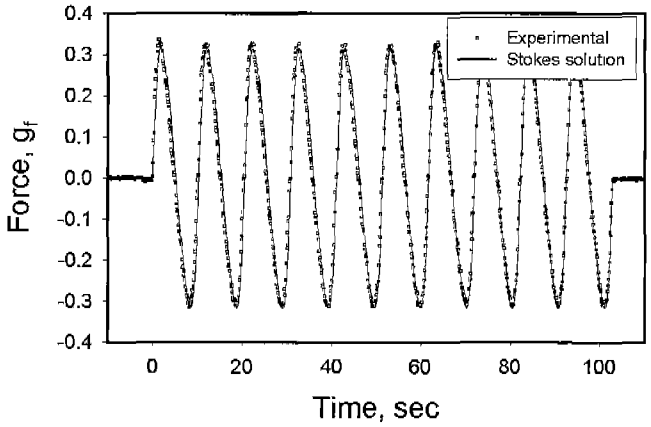

Fig. 7. The force exerted on the stationary sphere when the plate oscillates when Re = 0.65. The liquid is glycerin. The experimental data is almost perfectly fitted to the Stokes solution corrected for the wall effect, which validates the experimental technique. In this case, inertial effect is negligible.

the sphere to result in the abrupt increase in the force exerted on the sphere. As the plate continues to move down, the gap becomes larger and the force is reduced until the plate reaches the position of the maximum separation. As the plate changes the motion of direction, the sign of the force changes and the force continues to decrease (the absolute value increases) until the plate reaches the minimum distance position. In this experimental condition of slow movement and large minimum gap size, the experimental result is fitted almost perfectly to the asymptotic solution assuming Stokes flow. This result also verifies the validity of the experimental procedure. Also, the almost exact match to the Stokes flow implies that the inertia of

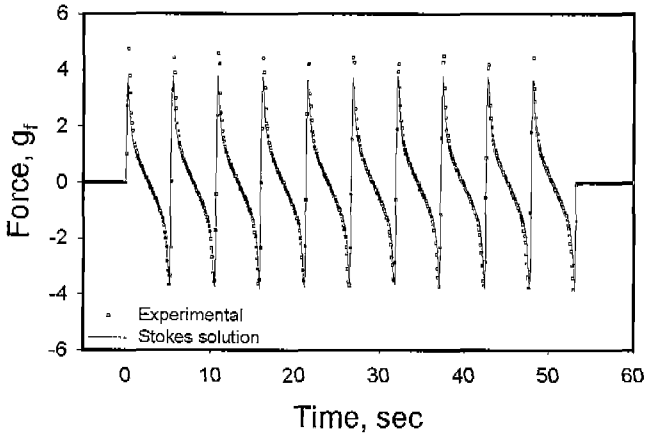

Fig. 8. The force exerted on the stationary sphere when the plate oscillates when Re = 1.36. The liquid is glycerin. The experimental data slightly deviates from the Stokes solution corrected for the wall effect when the wall moves down. In this case, inertial effect is not negligible.

bulk motion of liquid be neglected in this experimental condition. This is also expected from the magnitude of Re (= 0.65) here.

In Fig. 8, the force exerted on the stationary particle due to the oscillatory movement of the wall is plotted when the approach of the particle is 99.5% of the maximum gap size and the period is 5.27 seconds. In this case Re of the bulk motion is 1.36. It is noted that the maximum force when the plate begins to move down is substantially larger than the value predicted by the Stokes flow. If the motion of fluid in the gap is sufficiently slow so that Re is vanishingly small, the force should be symmetrical with respect to the position of the maximum separation between the plate and sphere as shown in Fig. 7. Hence the asymmetry observed in the experiment should be a deviation from the Stokes flow.

First of all, the deviation from the Stokes flow arises due to the unsteadiness of motion. The force due to the unsteady motion (oscillation) reaches the maximum when the distance between the particle and the wall passes the maximum or the minimum separations and it is given as follows (Clift *et al.*, 1978):

$$F_{osc} = \frac{V}{2}\rho\frac{dU}{dt} + 3\pi a^2\left[\frac{2\mu U}{\delta} + \delta\rho\frac{dU}{dt}\right] \tag{6}$$

where V is the volume of sphere, ρ is the density of liquid and $\delta = (2\mu/\rho\omega)^{1/2}$. According to Eqn. (6), when the period of motion is 5.27 sec, the difference between the maximum and the minimum forces is 0.14gram-force. This difference may not be negligible, but it cannot account for the large difference observed in the experiment. Also, the sign of F_{osc} is given such that it increases the absolute value of the maximum force for the movements in both directions. This force is symmetrical and hence cannot account for the asymmetry.

Usually the flow in the gap is considered as a lubricated squeezing flow while the inertia is neglected. We believe that the validity of this assumption needs to be reconsidered. The average Reynolds number at the gap of distance h can be estimated from the scaling analysis as follows. From the continuity equation, the average radial velocity scales as

$$V_r \approx U_z a/h \tag{7}$$

and then the Reynolds number based on the gap distance is

$$Re_{gap} \approx \frac{V_r h\rho}{\mu} = \frac{U_z a\rho}{\mu} \tag{8}$$

which is the same as the Reynolds number of bulk motion. In the above equation U_z and V_r are the average velocities along z and r directions, respectively. Even though Reynolds number based on the average gap distance and average velocity is small, the Reynolds number based on an instantaneous velocity could be much larger than this

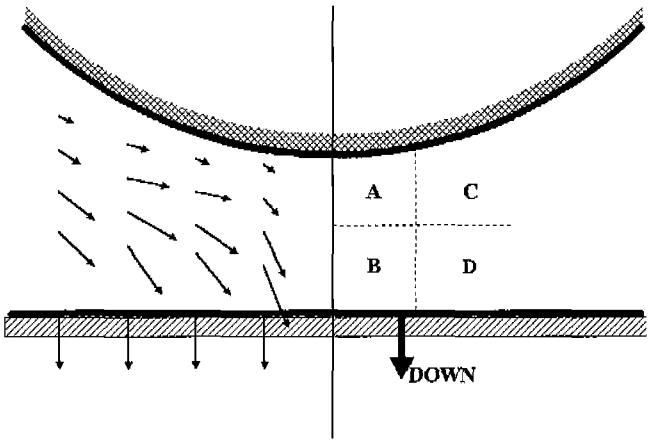

Fig. 9. Close view of the interstice region between the wall and the particle. Due to the sign change in the radial velocity gradient along the radial direction from the axis, the inertial effect is different in regions A, B, C and D, which results in the asymmetric as shown in Fig. 8 even in the case of Newtonian fluid.

value. This is because, when the sphere nearly touches the wall, the gap distance is almost singularly small. In this case the velocity is much larger than the average velocity, and hence the inertia may not be neglected. The effect of inertia could be estimated by examining the contribution of the inertial terms at some gap regions to the pressure distribution and the resultant force exerted on the sphere.

We first divide the gap into four regions as shown in Fig. 9. In regions A and B, v_r increases with r when the wall moves up while v_r decreases with r in regions C and D. The reverse will be true when the wall moves down. The force that the sphere senses is largely determined by the pressure values of regions A and C. These values can be determined by integrating the following r-component equation of motion:

$$\frac{\partial p}{\partial r} = \mu\frac{\partial^2 v_r}{\partial z^2} - \rho v_r\frac{\partial v_r}{\partial r} - \rho v_z\frac{\partial v_r}{\partial z} \tag{9}$$

We now consider the relative contribution of inertia terms in the above expression when the wall moves down. When the wall begins to move down, v_r becomes negative. In region A, due to the axisymmetry, v_r remains small while it has a large value in region C where by small or large, we mean only the magnitude. The fluid that is entrained from C is sucked along the z direction. $\partial v_r/\partial r$ is positive in regions A and C because v_r is negative and the magnitude becomes larger with increasing r. v_z is negative and small at A and C while it is negative and large at B and D. $\partial v_r/\partial z$ is small and positive at A because v_r itself is small and the velocity at the sphere surface is zero. $\partial v_r/\partial z$ is large and positive at B and D from the similar reasoning. To obtain p, the pressure gradient is integrated along the radial direction

and the force is obtained by summing up $p\,dA$ where dA is the surface element. dA is small at A and large at C considering the radius of each region. If we compare the terms considered above, we find that only the $-\rho v_r \times (\partial v_r/\partial r)$ term at region C has a positive and large contribution to the pressure gradient except the viscous term which is also positive. This contribution of the inertia term to the resultant force is roughly estimated to be about $\pi a^2 \times \rho v_r^2 \approx \pi a^2 \times \rho U_z^2 (a/h)^2$. This amounts to 0.96 gram-force when the experimental condition is chosen as in Fig. 8 and U_z is set to be $d\omega$. The extra force due to inertia is closely matches the experimental observation. This value shar- ply decreases as the gap distance increases and the force becomes matched to that of Stokes flow as shown in Fig. 8. Therefore it is concluded that the inertia plays a significant role when the average particle-wall separation is small and the frequency of collisions between particle and wall is large. This condition arises in the high shear flow of concentrated suspension.

When the plate moves up, from the similar reasoning, $v_r(\partial v_r/\partial r)$ and $v_z(\partial v_r/\partial z)$ have the opposite sign and offset each other approximately, hence no large deviation from the Stokes flow is observed. In Table 1 and 2, the sign and relative size of each term in Eqn. (9) are listed at regions A, B, C and D when the plate moves down and up, respectively.

In Fig. 10 the force exerted on the stationary particle due to the oscillatory movement of the wall in polymer solution is plotted when the period is 10 seconds. In this case the inertial effect should be small since it was already confirmed that the inertia is negligible with less viscous Newtonian liquid. When the wall moves toward the particle, the force exerted on the particle is smaller than the value predicted by the Stokes flow based on the zero-shear viscosity. The experimentally measured force is smaller due to shear thinning when the particle and wall are very close and the shear rate becomes extremely large. The reduction of force is about 35% which is almost the same as the viscosity reduction (See Fig. 7). The normal stress difference appears smaller than the viscous stress. When the period is 5.27 seconds and the approach is 99%, the force exerted on the particle is much different from the Stokes solution as shown in Fig. 11. It is also different qualitatively from the result shown in Fig. 7. The peak value is closer to the Stokes solution even though more shear thinning is pre-

Table 1. Sign and the relative size of the terms in Eqn. (9) in each region inside the gap when the plate moves down

	Region A	Region B	Region C	Region D
v_r	-, small	-, small	-, large	-, large
$\partial v_r/\partial r$	-	-	+	+
v_z	-, small	-, large	-, small	-, large
$\partial v_r/\partial z$	+, small	-	+, large	-
dA	small	Small	large	large

Table 2. Sign and the relative size of the terms in Eqn. (9) in each region inside the gap when the plate moves up

	Region A	Region B	Region C	Region D
v_r	+, small	+, small	+, large	+, large
$\partial v_r/\partial r$	+	+	-	-
v_z	+, small	+, large	+, small	+, large
$\partial v_r/\partial z$	-, small	+, small	-, large	+, large
dA	small	Small	large	large

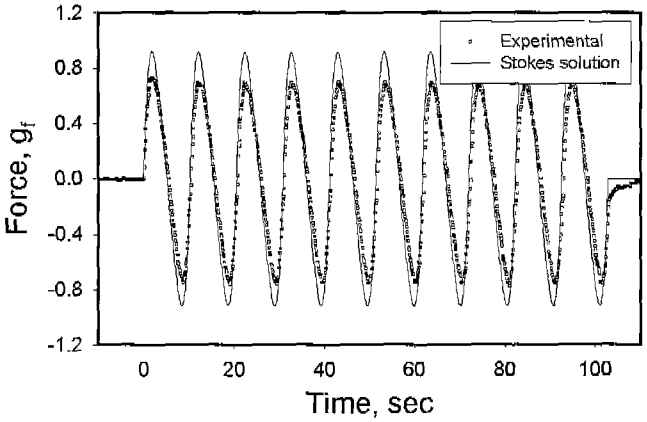

Fig. 10. The force exerted on the stationary sphere when the plate oscillates under the same condition as in the case of Fig. 7. In this case, the Reynolds number is smaller due to increased viscosity. The experimental data deviates from the Stokes solution corrected for the wall effect due to shear thinning when the sphere and the wall become close.

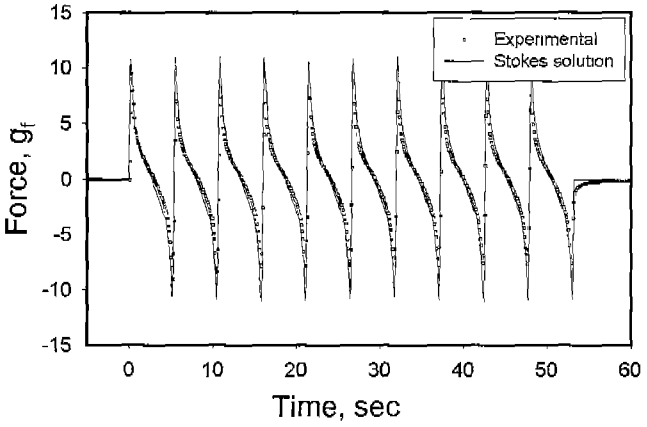

Fig. 11. The force exerted on the stationary sphere when the plate oscillates under the same condition as in the case of Fig. 8. In this case, the Reynolds number is smaller due to increased viscosity. In this case, all the non-Newtonian effects, shear thinning, non-zero normal stress difference and viscoelasticity affect the force between the particle and the wall.

dicted for this small gap problem than the wide gap problem considered in Fig. 10. This appears to be the effect of the first normal stress difference. The steep increase as the wall approaches the particle also reflects the second order dependency of N_1 with respect to shear rate. The profile does not have the symmetry with respect to the baseline of each cycle due to the viscoelastic nature of polymer solution.

The force at the smallest gap has the largest value for the first cycle and then it becomes smaller from the second cycle. This appears to be caused by the migration of polymer molecules from the interstice where the shear rate is extremely high. This also means that there is apparent wall-slip at the interstice region.

5. Concluding Remarks

The particle-wall interaction in suspension is a very complicated process governed by various factors: In Newtonian fluid, in addition to the viscous forces, fluid inertia plays an important role when the particle loading is high and shear rate is large. In polymer solutions, viscoelasticity, shear thinning and normal stress affect the particle-wall interaction together with the apparent wall-slip due to the migration and concomitant depletion of polymer molecules from the gap. To understand more on the physics of particle-wall interaction, we need more researches on this subject with fluids of differing rheological behavior.

Acknowledgments

The authors wish to acknowledge the financial support from the Korea Science and Engineering Foundation (Project Number: 981-1104-016-2).

References

Barnes, H.A., J.F. Hutton and K. Walters, 1989, An introduction to rheology, Elsevier, Amsterdam.

Brunn, P., 1977, Interaction of spheres in a viscoelastic fluid, *Rheologica Acta* **16**, 461-475.

Clift, R. J.R. Grace and M.E. Weber, 1978, Bubbles, drops and particles, Academic Press, New York.

Dontula, P., C.W. Macosko and L.E. Scriven, 1999, Model elastic liquids with water-soluble polymers, *AIChE J.* **44**, 1247-1255.

Folkersma, R., H.N. Stein and F.N. van de Vosse, 2000, Hydrodynamic interactions between two identical spheres held fixed side by side against a uniform stream directed perpendicular to the line connecting the spheres centers, *Int. J. Multiphase Flow* **26**, 877-887.

Happel, J and J. Brenner, 1983, Low Reynolds number hydrodynamics, Nijhoff, Dordrecht.

Huang, P.Y., J.Feng, H.H. Hu and D.D. Joseph, 1997, Direct simulation of the motion of solid particles in Couette and Poiseuille flows of viscoelastic fluids, *J. Fluid Mech.* **343**, 73-94.

Jefri, M.A. and A.H. Zahed, 1989, Elastic and viscous effects on particle migration in plane-Poiseuille flow, *J. Rheol.* **33**, 691-708.

Kim, C., 2001, Migration in concentrated suspension of spherical particles dispersed in polymer solution, *Korea-Australia Rheol. J.* **13**, 19-27.

Kim, S.K., M.S. Han and C. Kim, 2000, Hydrodynamic diffusion of spherical particles in polymer solution undergoing Couette flow, *Rheologica Acta,* **39**, 495-502.

Kim, S. and S.J. Karrila, 1991, Microhydrodynamics, Butterworth-Heinemann, Boston.

Larson, R.G., 1992, Instabilities in viscoelastic flows, *Rheol. Acta* **31**, 213-263.

Patankar, N.A. and H.H. Hu, 2001, Rheology of suspension of particles in viscoelastic fluids, *J. Non-Newt. Fluid Mech.* **96**, 427-443.

Phillips, R.J., R.C. Armstrong, R.A. Brown, A.L. Graham and J.R. Abott, 1992, A constitutive equation for concentrated suspension that accounts for shear-induced particle migration, *Phys. Fluids* **A4**, 30-40.

Shaqfeh, E.S.G., 1996, Purely elastic instabilities in viscometric flows, *Annu. Rev. fluid Mech.* **28**, 129-185.

Solomon, M.J. and S.J. Muller, 1996, Flow past a sphere in polystyrene-based Boger fluids: the effect on the drag coefficient of finite extensibility, solvent quality and polymer molecular weight, *J. Non-Newt. Fluid Mech.* **62**, 81-94.

Tehrani, M.A., 1994, An experimental study of particle migration in pipe flow of viscoelastic liquids, *J. Rheol.* **40**, 1057-1077.

Yang, S.M. and O.O. Park, 1997, Principles of the flow of microstructured fluid (in Korean), Mineumsa, Seoul.